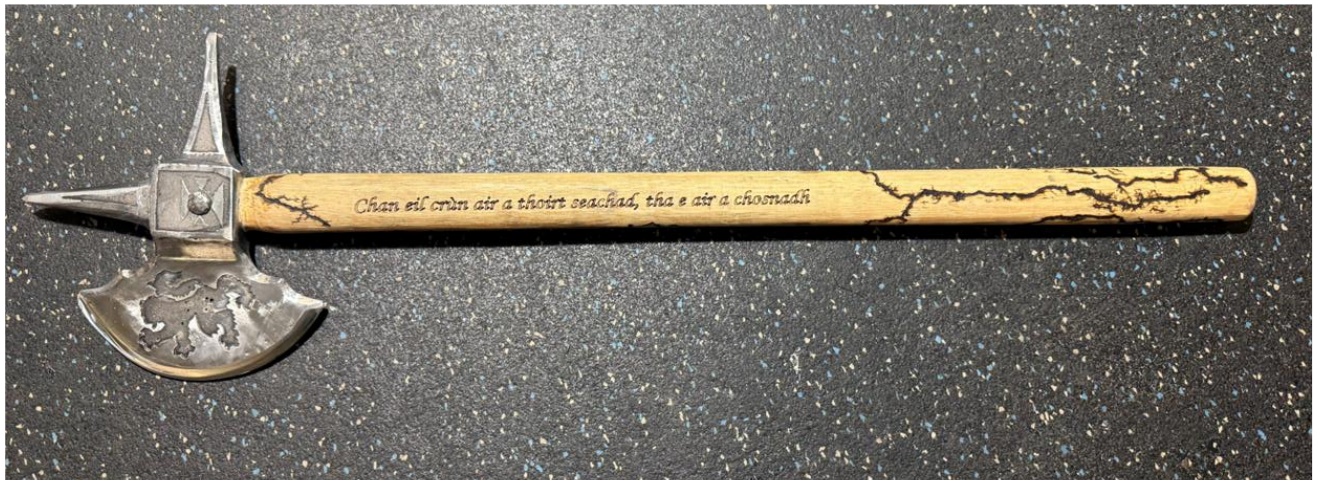
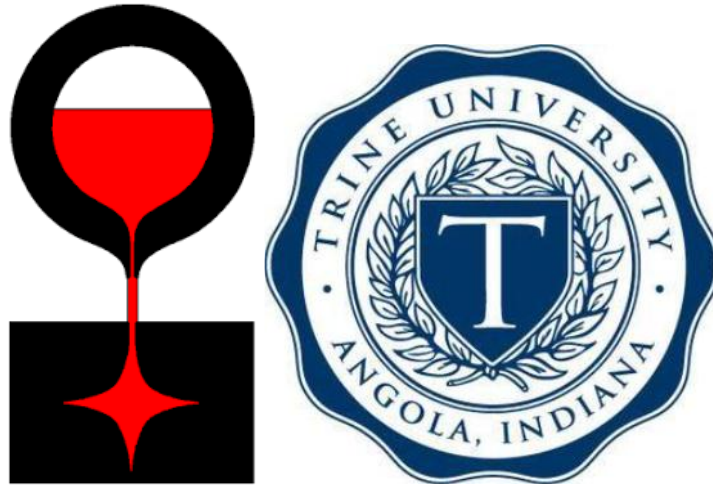


SFSA Cast In Steel 2026 – Horseman’s Axe

Technical Report

Trine University – Steel Thunder



Team Members:

Dakota Carter, Sean Kohloff, Peter Osborne, Garrett Spahr, and Kelly Valle

Advisor(s) Name:

Dr. Darryl Webber, Dr. Rizacan Sarikaya, and Mr. Joseph Thompson II

Foundry Partner:

Bahr Brothers Manufacturing Inc.

1. Executive Summary

The 2026 Steel Founders' Society of America (SFSA) Cast in Steel competition requires undergraduate teams to design and cast a functional horseman's axe with three implements: a blade, pick, and spike. Teams must do this while meeting overall limits of less than 1.5 kilograms in mass (3.3 pounds) and 800 millimeters in length (31.5 inches). Additionally, the competition requires a technical report of no more than ten pages and a five-minute project video. In their own words, the "SFSA has created this competition to encourage students to learn about making steel products using the casting process and applying the latest technology available," (Steel Founders' Society of America, 2026). The purpose of this is to inspire, educate, and provide up-and-coming members of the casting industry with real-world experience on how the steel casting process can be used in creative ways to make quality products.

Our Trine University team created a historically inspired, competition-compliant design that we optimized through decision matrices, finite element analysis (FEA), and casting simulations, followed by validating the design through structured testing. The final axe incorporates a curved cutting blade, a straight pick for armor engagement, and a central spike for thrusting. It is cast in our self-made metallurgical mix of AISI 4140 steel and heat-treated to approximately 56 HRC to deliver edge retention, toughness, and manufacturability. Iterative improvements to gating increased our predicted casting yield from about 33% to about 58%, while reducing porosity risk in key areas. The completed process included 3D-printed match plates, green-sand molding, induction melting, oil quenching and tempering, precision grinding, nondestructive testing, sample material testing, and performance-based testing that aligns both with what SFSA evaluators will examine, as well as the most extreme usage scenarios possible.

2. Historical Background and Weapon Context

The SFSA competition references the legendary horseman's axe associated with Robert the Bruce, King of Scotland. He most famously used this weapon at the Battle of Bannockburn in 1314 to strike down the English knight Henry de Bohun with a single blow to the head, cleaving right through his helmet (Marshall, 1906). Surviving historical illustrations and descriptions show multiple variations of the weapon, including versions with a single blade and those featuring combinations of blade, pick, and spike like the competition requirements. These artifacts typically display compact heads with a handle slightly longer than Bruce's forearm, such as in Figure 1. Despite Robert the Bruce's axe being a primary weapon in its most famous use, this type of weapon was typically a secondary to a mounted knight's lance or pole weapon (Abbott & Baker, 2025). Being mounted severely limited a knight's ability to use both hands to control the axe, so it was typically wielded one-handed. This made weight, size, and handle indexing extremely important, as a warrior would have to be able to precisely draw the axe and swing one of its implements at enemies within a moment's notice. Too heavy or long, and weapon control would be severely diminished. Too round of a handle, and the wrong face of the axe could be used, severely diminishing the effectiveness of a strike.

Our team drew from historical weapon forms to influence the geometry and functional intent of the modern design, while adapting dimensions and features for performance, durability, and safe operation. For instance, our final axe head shape closely mimicked the relative size of the blade shown in Figure 2, which was aimed at beating the maximum weight requirement. However, we chose to incorporate a straighter pick, as is shown in Figure 3 and Figure 4, to simplify the design and speed up secondary processing. Historical functionality was also considered as design ideas were evaluated in our decision matrices. A top spike was not useful to a mounted knight in most situations, as a one-handed lunge would

have had little power behind it (Abbott & Baker, 2025). For this reason, the large spike design seen in the historical examples was avoided to save weight for the other implements and increase practicality. The wooden versus metal handle choice was considered for accuracy as well. In most depictions the team found, Bruce's axe has a wooden shaft, such as in Figure 5. This, along with weight, contributed to selecting a wooden handle in the design stages.

3. Competition Requirements and Program Constraints

The competition enforces strict limits on the overall mass, overall length, and required implements of the axe. It also mandates partnership with a foundry in industry, this 10-page technical report, a five-minute video, and a testing sequence that simulates medieval combat applications. Internally, our team worked under constraints involving foundry safety compliance and a regular weekly pouring schedule in aluminum, brass, iron, and steel for targeted mold modifications. We set additional performance objectives, including achieving a blade sharpness target of around BESS 250, obtaining a hardness of roughly 58 HRC at the edge after heat treatment, maintaining an edge angle below 25 degrees, and performing extensive nondestructive inspections prior to shipment. The full extent of these criteria can be seen tabulated in Table 1.

4. Design Objectives and Decision Framework

To manage the complexity of the weapon, the team divided the design into seven subsystems: handle, axe blade curvature, axe blade edge grind, axe blade side profile (head shape), axe head to handle connection type, pick curvature amount, and steel alloy. Ideas were evaluated using weighted decision matrices, which varied per the requirements of the individual subsystem. An example matrix for the handle wood selection can be seen in Figure 7.

We selected wood for the handle based on mass, manufacturability, and historical authenticity, and ultimately chose ash for its relevance to medieval Scotland, good mechanical properties, and workable density. However, limits to the availability of ash handles and quality ash wood ended up forcing the team to use a hickory version in the final iteration. A commercially available sledgehammer-style blank provided a consistent starting point for shaping, with the final geometry being more rectangular for slightly better indexing. This straight handle style was common throughout our research and matched what we saw in Figure 1, Figure 2, Figure 3, Figure 4, Figure 5, and Figure 6.

A curved blade was chosen to maximize cutting capability, while a wrap angle of less than 180 degrees reduced mass and grinding time without sacrificing structural behavior. A convex edge grind offered the best combination of durability and sharpness retention based on our research (A. G. Russell Knives, 2025) (Grönsfors Bruk Sweden, n.d.) (User, 2010) (Woox, 2025). FEA further validated this design choice after evaluating models of each grind type in Table 2.

FEA comparisons between straight and curved pick geometries in Figure 8 and Figure 9 showed lower stresses and reduced deformation in straight designs, informing our final selection for this as well. A straight pick was also considered to be much easier to grind and polish with Trine's available tools, which was considered a functional advantage.

For the head-to-handle connection, a single pinned and glued joint was chosen for its simplicity, reliability, and limited added mass. Finally, AISI 4140 steel was selected due to its excellent heat-treat response, machinability, castability, and mechanical performance.

5. Final Design Description

The completed design, seen in Figure 10, Figure 11, Figure 12, and Figure 13, integrates a curved blade, a straight tapered pick, and a centered top spike. The top spike comes to a sharp point for thrusting, the pick comes to a dull point for armor penetration, and the blade features a convex grind for superior durability and edge retention. There are decorative radii on the rear of the blade extrusion as well. The blade neck transitions smoothly to the socket to minimize stress concentrations and provide robust load transfer during impact. The head attaches to the handle using a through-pin that passes through both the axe head and the fitted wooden handle. The axe head is cast as a single solid piece of steel, taking advantage of the greensand casting process and corresponding core to create the tightly toleranced geometry for the handle hole while still allowing for large cross sections of material at the base of the spike and pick.

The handle is shaped from a sledgehammer handle blank that was sanded down and sealed with boiled linseed oil, a traditional wood finish that is both correct for the period and helps protect the handle from moisture (Mussey, 2023). The length was adjusted by handling prototypes in a manner similar to the one-handed mounted use consistent with historical examples and the competition requirements discussed in the SFSA informational videos (Abbott & Baker, 2025). JB Weld epoxy fills minor gaps in the head–handle interface and provides moisture protection, while the peened pin locks the assembly mechanically.

Scottish Gaelic, one of the primary languages of Robert the Bruce, was used to laser-cut the inscription of “Chan eil crùn air a thoirt seachad, tha e air a chosnadh,” into both sides of the upper handle, as seen in Figure 14 (Brown, 2018). This quote from Robert translates to “A crown is not given, it is earned,” which the team believed both sounded cool and embodied the spirit of the Cast in Steel competition (The Bruce Festival, 2025). Many teams can claim to have the best axe or the most skilled members, but only by passing the rigorous competition testing can the winners be crowned.

Also on the handle is a lightning bolt pattern that was burned in using high-voltage electricity. These Lichtenberg figures, as they are scientifically labeled, are pictured in Figure 15 and are a nod to the team’s name, Steel Thunder. Towards the end of the handle the concentration of these patterns was increased to assist with grip, providing a functional purpose as well.

Etching and bluing were also incorporated into the final design of the axe head, as seen in Figure 13. Two triangular etched and blued areas add highlights to the pick and spike. The design in the main body roughly resembles multiple depictions of Robert the Bruce’s shield and is centered on both sides about the peened-over pin (ScotClans.com, 2026). The final etch and blued areas are on the sided of the blade and feature a lion rampant, which is part of the Bruce Clan’s coat of arms and was commonly associated with Scottish royalty in the 13th Century as well (ScotClans.com, 2026).

The final weight of the completed axe was 1.25 kilograms (2.75 pounds), falling 0.25 kilograms (0.55 pounds) under the competition maximum weight limit. The material composition was confirmed via arc spectrometer testing to match AISI 4140 tool steel, as seen in Table 3 and Figure 16, and the edge hardness was confirmed via hardness testing files to be between 55 and 57 HRC. This is slightly lower than the team initially desired but should still perform well. The blade sharpness was measured to be an average of 256 on the BESS scale with a sample of ten measurements. The final length of the handle surface is 22.5 inches, with a full length of 27.75 inches from the tip of the spike to the end of the handle. The blade to pick tip measurement is 8 inches, with a blade height of 5.5 inches. The pin used is made of a rod of an unknown steel type and is a diameter of 0.3 inches.

6. Materials and Heat Treatment

AISI 4140 steel was chosen because its carbon, chromium, manganese, and molybdenum content allows it to achieve the team's desired combination of hardness, toughness, and castability (AZO Materials, 2019). Specifically, it is heat treatable to HRC readings upwards of 60, has very high tensile and ultimate strengths, and is still machinable (MatWeb, 2025).

The heat treatment process plan began with normalizing at 870°C for 50 minutes to refine the microstructure and reduce residual stress. In this process, the first 15 to 20 minutes was done while the furnace was heating up, and the remainder was done at full temperature.

The blade was then austenitized at 845°C using refractory cement around the main body to keep it cooler than the spike tips and blade edge, as shown in Figure 17. This was done to help keep the socket and core of the axe head more tough and ductile than the tool edges and points. The heating cycle was identical in all but temperature to the normalization process.

The axe was then quenched in a large volume of canola oil to form martensite along the edge, which has exceptional wear resistance and hardness properties (Tuckey, 2022). A final temper at 200°C, with 15 minutes of heating up and 2 hours at full temperature, reduced brittleness and was designed to produce the target edge hardness of about 58 HRC while maintaining toughness through the core, especially in the pick and socket regions. During all steps of the process a boron nitride coating was used on the exposed metal and sacrificial charcoal was placed in the furnace to prevent decarburization and scaling as well.

This process was designed by using many different charts and diagrams from the ASM Handbook Volume 4: Heat Treating and notes from the team's classes with FEF Key Professor and advisor Dr. Webber. One such diagram can be seen in Figure 18, which depicts the tempering temperature versus hardness and toughness of 4140 tool steel. However, during prototyping the team found that the edge did not get as hard as expected when using these references. After consulting with Dr. Webber, the team modified the process to have an austenitizing temperature of 900°C, which produced better results.

7. Casting Process and Manufacturing

The team was restricted in the selection of a casting process, as Trine is primarily set up for green sand casting. 3D-printed split patterns for this process with allowances for shrinkage, printer tolerance, and machining stock were used to create match plates like those in Figure 19. Induction melting using the in-house furnace enabled clean, controlled alloying using primarily recycled steel punchings, in addition to amounts of additives that were calculated using a team-built composition calculator code.

MAGMA simulations revealed areas susceptible to porosity and poor solidification during early design iterations, especially around the core, as seen in Figure 20 and Figure 21. Adjustments to risers, runners, and venting gradually improved directional solidification, raising estimated casting yield from roughly 33% to roughly 58% in the final version depicted in Figure 22 and Figure 23. MAGMA was also used to optimize the core design. Initially the mold was showing a high chance of porosity at the base of the blade and spikes, so the team simulated putting a chill inside of the core to help reduce hot spots around the core. Simulation results were promising, so a physical test was done as well, which led to a cylindrical steel rod being put inside of the final cores. Early practice pours in aluminum and brass verified the gating concepts before final ferrous production, leading to no changes being made once steel was being poured. The cores were made of a Chem-Bond no bake system and resembled the one shown in Figure 24. After pouring, castings cooled for an hour in the mold before break-out, followed by removal of gating, surface

cleaning, and machining of spectrometer button samples to confirm the chemical compositions before heat treatment.

8. Secondary Processing, Assembly, and Finish

After heat treatment, the blade edge was shaped using a convex primary grind and refined through successive abrasive belts before being hand-finished and polished. This geometry resisted rolling and chipping under impacts involving wood, metal, or ice in simulations of a blade speed of 150 miles per hour (approximately 67 meters per second), as seen in Figure 25. This is far above the impact speeds the axe would see in use, which validated the design with a safety factor of just about two (Inkster, Murphy, Bower, & Watsford, 2011). The handle was fitted precisely into the hole on the casting, epoxied, drilled, and pinned using a steel rod that was peened over on the ends. The finished head then received a wipe-over with light tool oil to resist rust. The handle was given three coats of boiled linseed oil, which was diluted with two parts mineral spirits per the manufacturer's instructions. The BLO was wiped on, let to soak in for five to 10 minutes, and the excess was wiped away before the final dry time. Each coat was given a drying time varying from 18 to 24 hours, depending on the initial absorption of the wood.

9. Simulation, Testing, and Verification

As previously mentioned, structural and dynamic finite element analysis using ANSYS software was performed to evaluate stress on the blade, pick, and pinned joint at angular velocities representative of competition impacts. Simulations showed that the straight pick option had lower stresses and deformation than curved alternatives, validating our design matrix conclusions.

Mechanical testing included hardness measurements across the edge and main body with a hardness testing machine and hardness testing files, which measured in at 56 HRC on the edge and 32 HRC on the main body. Sharpness testing was performed using a BESS testing kit and was found to be 256 after a sample of 10 data points.

The measurements obtained for impact energy absorption were obtained via Charpy impact method and were compared directly to true AISI 4140 samples that were on hand. The true samples of 4140 averaged 46.2 foot-pounds absorbed with a standard deviation of 1.605 foot-pounds, and the cast 4140 averaged 39.4 foot-pounds absorbed with a standard deviation of 22.726 foot-pounds. The full data set is listed in Table 4. As seen in Figure 26, the true 4140 samples failed with obvious ductile fractures, while the cast 4140 bars all failed in more of a brittle mode. This was likely due to the true 4140 specimens being rolled during production, which led to more directional grain flow than the cast bars' more random and dendritic structure. Also, the rolling process would have improved toughness and helped to eliminate microporosity in the microstructure, which would have been a major factor in crack initiation for the cast bars.

With the help of Metal Technologies Auburn, tensile tests were also performed on representative samples. The samples pulled showed a tensile strength of 91,725 psi and a yield strength of 85,000 psi, compared to a 4140 standard of 95,000 psi for tensile strength and 60,200 psi yield strength Figure 27.

The Auburn, Indiana, Linamar Light Metals casting plant provided additional support with X-ray imaging on one of their in-house Bosello units, helping the team identify porosity in the final castings and to identify areas needing ground and weld repaired. This is shown in Figure 28, Figure 29, Figure 30, and Figure 31. This also validated the MAGMA simulations and proved that a low to nonexistent amount of porosity was present where it was designed out of the molds Figure 32.

Functional testing of a second axe prepared the team for SFSA evaluations through controlled chopping, slicing, piercing, and ice-impact trials like in Figure 35. The controlled swing of a garage door spring powered testing rig provided repeatable impact energies for consistent edge-retention evaluation, as shown in Figure 33 and Figure 34. The garage door spring sizing was done using a rough estimate of the energy required to lift a garage door and the energy required to swing an axe. For a 200-pound door, lifting 3.5 feet requires about 952 Joules of energy, which is calculated using the gravitational potential energy equation, $U = mgh$. This corresponds to about 8 turns while winding the spring. When swinging a 3-pound axe, the equation for kinetic energy is used instead, $E_k = \frac{1}{2}mv^2$. The average baseball swing speed is approximately 30 m/s, which is likely more powerful than a single-handed axe swing, but provided a solid base for approximation. At that velocity, the axe has a kinetic energy of 612 Joules. This is approximately 64% of the energy expended by the garage door spring, meaning that the fully wound spring could successfully subject the axe to a stronger-than-human force.

Edge retention on the second axe turned out to be successful during a cantaloupe slice, wood dowel chop, 1-inch by 6-inch board chop, ice block chop, 18-gauge steel plate chop, and 16-gauge steel pipe chop. Throughout all the tests, the axe did significant damage. There was a slight dulling of the axe edge, but no chipping occurred and the axe still was sharp enough to cut after testing Figure 36. The garage door spring mechanism was also used to test the pick on ice, plywood, cantaloupe, and steel plate, with successful punctures on all three without the axe incurring any damage, which can be seen in Figure 37 and Figure 38. All in all, this testing proved the effectiveness of the weapon and left the team with the delicious cantaloupe in Figure 39 and the full trash can in Figure 40.

10. Obstacles Faced and Problems Solved

In addition to the core chill, porosity elimination, and heat treatment tuning, the team faced other challenges on the road to a complete axe. Two major furnace malfunctions delayed steel pours from November to Mid-January. By consulting with the lab manager and some outside help, the furnace was up and running in the nick of time, and the team worked at an accelerated pace to once again be ahead of schedule.

The team also ran into multiple ladle cracking issues after the furnace was fixed, which caused relines to be necessary multiple weeks in a row. Once again, doubling down on the issue and bringing in outside help when needed allowed the team to reduce the issue's impact on the final delivery date.

11. Project Management and Execution Summary

A structured framework using Gantt charts, PERT diagrams, and a work breakdown structure guided our scheduling and role assignments. Our progress moved through Concept, Critical, and Final design stages, with aluminum and brass casting trials conducted early on to reduce the risk of a bad mold design. Each of the team members had responsibilities fit to his or her individual strengths to keep our progress consistent in all areas throughout the project, and when challenges arose the team stepped up to help each other.

Dakota was designated project manager and in doing so coordinated scheduling and led meetings. He managed alloy research and oversaw MAGMA simulations, which he used to optimize our gating and risers to eliminate porosity and improve yield. Etching, bluing, and Lichtenberg figures also fell under his purview as time went on, ensuring a good-looking final product.

Garrett was in charge of historical research, which was essential for the initial design phase. He also collaborated with Sean to make match plates, performed periodic sand testing, and oversaw mold and core preparation for every pour, which directly impacted our castings every week. He also managed the creation of the project video for competition, which was a significant portion of the project work.

Peter was the best at using ANSYS, so he was put in control of the group's FEA simulations. He also quarterbacked pour days and calculating out our alloying adjustments for each pour, which was instrumental to our final material properties. Secondary processing such as grinding, polishing, and weld repair also fell under his oversight, which was critical to the final edge geometry and performance of the axe.

Sean primarily oversaw all our testing, which included personally designing and building the garage door spring test rig. He was also in charge of the group's CAD and 3D printing, which was crucial for match plate and core box creation. On pour days, he ran the hydraulics for the furnace and was one of the most efficient molders as well. Without him, the rest of the group would have been unable to complete their tasks.

Kelly joined the team after the winter holidays, so she was a jack of all trades. She primarily helped with finishing on our additional axe heads and on obtaining the project video content. She also started to design a new camera rig for future years of Trine's Cast in Steel teams and will serve as a bridge member for getting next year's team up to speed on the complexities of the competition.

12. Final Specifications and Conclusion

The axe incorporates a curved blade, straight pick, and central spike, remains below the 800-millimeter length limit, and maintains mass below 1.5 kilograms. It is cast from AISI 4140 steel and was heat-treated to reach about 56 HRC at the cutting edge. Quality checks included performance simulations, arc spectrometer analysis, hardness testing, X-ray imaging, Charpy testing, tensile bar pulls, and a rigorous and destructive cycle of testing. All said, Steel Thunder's design meets all SFSA requirements and is prepared for evaluation at the 2026 competition.

The final design successfully blended historical inspiration with strong engineering optimization, leading to a competition-ready horseman's axe that will meet functionality requirements. Despite furnace troubles, core issues, and life getting in the way, the team came together to learn from mistakes, resolve issues, and submit a final product we are proud of.

13. Acknowledgments

We would like to thank Dr. Darryl Webber and Dr. Rizacan Sarikaya for advising, along with Mr. Joe Thompson II and Trine University's AFS underclassmen for their assistance with alloying, materials, and processing guidance. We would also like to thank Don Carter, Htet Khaing, and the rest of Linamar Light Metals – Auburn for their assistance with X-ray scanning our cast axe heads, which was instrumental in selecting the correct axe for competition and for guiding weld repair. We would like to thank Kramer Pursell and Metal Technologies Auburn for performing our tensile testing and providing no-bake tensile bar molds as well, which was a large part of material testing. Finally, we would like to thank Bahr Brothers Manufacturing Inc. for agreeing to be our industry partner, even though we ran into scheduling difficulties that prevented our teams meeting face to face before the submission of this report.

14. Bibliography

- A. G. Russell Knives. (2025). *Blade grinds*. Retrieved from <https://agrussell.com/knife-articles/blade-grinds>.
- Abbott, B., & Baker, D. (2025, July 29). Cast in Steel Horseman's Axe Expert Discussion. (R. Monroe, Interviewer)
- Art Institute Chicago. (2026). *Horseman's Axe*. Retrieved from [artic.edu: https://www.artic.edu/artworks/116956/horseman-s-axe](https://www.artic.edu/artworks/116956/horseman-s-axe)
- Art Institute of Chicago. (n.d.). *Horseman's Axe [Axe]*. Retrieved from [artic.edu: https://www.artic.edu/artworks/116956/horseman-s-axe](https://www.artic.edu/artworks/116956/horseman-s-axe)
- AZO Materials. (2019, December 18). *AISI 4140 Alloy Steel (UNS G41400)*. Retrieved from AZOM.com: <https://www.azom.com/article.aspx?ArticleID=6769>
- Bonhams. (2012, April 18). *European Horseman's Axe*. Retrieved from Bonhams: <https://www.bonhams.com/auction/19793/lot/58/a-european-horsemans-axe/>
- Brown, D. C. (2018, June 21). *Robert the Bruce: Earl, outlaw, king*. Retrieved from TheHistoryPress.co.uk: <https://thehistorypress.co.uk/article/robert-the-bruce-earl-outlaw-king/>
- Grönsfors Bruk Sweden. (n.d.). *Sharpening your axe*. Retrieved from https://www.gransforsbruk.com/en/info/sharpening_your_axe/
- Hassall, J. (2025, September 25). *Robert de Bruce strikes and kills Sir Henry de Bohun with his axe in single combat before the Battle of Bannockburn on 23rd June 1314*. Retrieved from BritishBattles.com: <https://www.britishbattles.com/scottish-war-of-independence/battle-of-bannockburn/>
- Heritage Images (n.d.). Robert the Bruce kills Sir Henry de Bohun, Bannockburn Print, 1314. <https://www.mediastorehouse.com/heritage-images/robert-bruce-kills-sir-henry-bohun-15138818.html>. Media Storehouse. Retrieved from <https://www.mediastorehouse.com/heritage-images/robert-bruce-kills-sir-henry-bohun-15138818.html>
- Incitatus. (2014, October 14). *File:Horseman's axe - 1475.jpg*. Retrieved from Commons.Wikimedia.org: https://commons.wikimedia.org/wiki/File:Horseman%27s_axe_-_1475.jpg
- Inkster, B., Murphy, A., Bower, R., & Watsford, M. (2011). Differences in the kinematics of the baseball swing between hitters of varying skill. *Medicine and science in sports and exercise*, 43(6), 1050-1054.
- Marshall, H. E. (1906). Chapter XLI. Robert The Bruce - How Sir Henry de Bohun met his Death. In *Scotland's Story*. London: T. C. & E. C. Jack, Ltd. Retrieved from <https://electricScotland.com/history/story/chapter41.htm>
- MatWeb. (2025, September). *MatWeb Search: AISI 4140*. Retrieved from MatWeb.com: <https://matweb.com/search/QuickText.aspx?SearchText=AISI%204140>
- Mussey, R. D. (2023, April 6). *Old Finishes*. Retrieved from JourneymansJournal.wordpress.com: <https://journeymansjournal.wordpress.com/2023/04/06/old-finishes-2/>
- Plunger, J., Cory, J., & Lilley, J. (2025, July 31). Cast in Steel - Best Casting - How to be successful - Expert Discussion. (R. Monroe, Interviewer)
- ScotClans.com. (2026, February). *Clan Bruce Crest & Coats of Arms*. Retrieved from ScotClans.com: <https://www.scotclans.com/blogs/clans-b3/clan-bruce-crest-coats-of-arms#:~:text=Crest%20Description:,Brudenell%2DBruce%20coat%20of%20arms>
- Steel Founders' Society of America. (2026, January). *2026 Competition*. Retrieved from CastinSteel.net: <https://www.castinsteel.net/2026-competition>
- Steel Founders' Society of America. (2026, February). *Frequently Asked Questions*. Retrieved from CastinSteel.net: <https://www.castinsteel.net/frequently-asked-questions>
- The Bruce Festival. (2025). *Robert The Bruce Quotes*. Retrieved from TheBruceFestival.com: <https://www.thebrucefestival.com/robert-the-bruce-quotes/>
- Tuckey, S. (2022, June 19). *What Is Martensitic Steel Used in Kitchen Knives?* Retrieved from KoiKnives.com: https://www.koiknives.com/blogs/japanese-knives/what-is-martensitic-steel-used-in-kitchen-knives?srsId=AfmBOotoX8qYgJy_itgfbdJfzvYR8B7JkechX2D97k1TCZmS_nl6Wac
- User, B. (2010, February 2). *Best axe edge geometry [Online Forum Post]*. Retrieved from bladeforums.com: <https://www.bladeforums.com/threads/best-axe-edge-geometry.725348/>
- usmcpop. (2018, November 5). *Question about welding 4140 steel and embrittlement*. Retrieved from [weldtalk.hobartwelders.com: https://weldtalk.hobartwelders.com/forum/equipment-talk/general-welding-questions/702146-questions-about-welding-4140-steel-and-embrittlement](https://weldtalk.hobartwelders.com/forum/equipment-talk/general-welding-questions/702146-questions-about-welding-4140-steel-and-embrittlement)
- Woox. (2025). *Sharper isn't always better: Understanding the edge requirements of axes*. Retrieved from [wooxstore.com: https://wooxstore.com/blogs/woox-journal/sharper-isn-t-always-better-understanding-the-edge-requirements-of-axes](https://wooxstore.com/blogs/woox-journal/sharper-isn-t-always-better-understanding-the-edge-requirements-of-axes)

15. Appendix of Figures

Table of Figures

Figure 1. A depiction of Robert the Bruce wielding his axe at the Battle of Bannockburn (Images).	11
Figure 2. A horseman's axe with a small blade and head size (Bonhams, 2012).	11
Figure 3. A horseman's axe on display in the Art Institute of Chicago (Art Institute Chicago, 2026).	11
Figure 4. An example of a horseman's axe with a large top spike (Incitatus, 2014).	12
Figure 5. Robert the Bruce breaking his wooden handled axe while striking Sir Henry de Bohun (Hassall, 2025).	12
Figure 6. A wooden handled horseman's axe at the Art Institute of Chicago (Art Institute of Chicago, n.d.).	13
Figure 7. An example of one of the team's selection matrices.	14
Figure 8. Finite element analysis during impact for the deformation of a curved pick.	16
Figure 9. Finite element analysis during impact for the deformation of a straight pick.	16
Figure 10. The CAD drawing of the final design, including preliminary dimensions.	17
Figure 11. A view of the computer model for the axe design.	17
Figure 12. The full completed axe.	18
Figure 13. The etched, blued, and polished axe head.	18
Figure 14. The axe handle inscription.	19
Figure 15. The Lichtenberg figures that were burned into the handle of the axe.	19
Figure 16. The arc spectrometer sample button and the data collection sheet for the final casting run in 4140 steel.	20
Figure 17. The refractory coating on the just-quenched axe head.	21
Figure 18. The tempering temperature versus hardness and toughness diagram (usmcpop, 2018).	21
Figure 19. The match plate for the final gating design.	22
Figure 20. The porosity simulation in MAGMA, showing a higher likelihood of porosity on the upper half of the casting around the core.	22
Figure 21. The solidification time for the MAGMA simulation of the final mold design, showing hot spots around the core.	23
Figure 22. The final gating for the axe head, including two open air risers, a direct feed riser, and an arc spectrometer button.	24
Figure 23. An aluminum pour of the final gating iteration before degating and removal of the core sand.	24
Figure 24. The core and core box for an early iteration of the axe.	25
Figure 25. The simulated total deformation of the axe under a 150 mile per hour impact with an ice block.	26
Figure 26. the Charpy impact test specimens, with "true" 4140 on the left and cast 4140 on the right.	27
Figure 27. The stress-strain curve for one of the tensile bars pulled by Metal Technologies Auburn.	28
Figure 28. The MAGMA simulation of the final gating, depicting the nearly eliminated chances of microporosity in the final casting.	32
Figure 29. The testing rig chopping a piece of 16-gauge steel pipe.	33
Figure 30. the testing rig chopping an 18-gauge steel plate.	33
Figure 31. Hand testing the axe against the 18-gauge steel plate.	34
Figure 32. The second axe's blade after destructive testing, which showed slight dulling and rollover.	34
Figure 33. The second axe's pick after destructive testing, which showed no damage.	35
Figure 34. Garrett enjoying fresh axe-sliced cantaloupe after successful destructive testing.	36
Figure 35. the trash can full of wood and cantaloupe scraps after destructive testing.	36

Table of Tables

Table 1. The engineering requirements for the Steel Thunder team.	13
Table 2. Depictions of each edge grind type considered for the axe.	15
Table 3. The percent composition ranges for AISI 4140 steel versus the final casting composition.	19
Table 4. The raw data from the Charpy impact testing.	27



Figure 1. A depiction of Robert the Bruce wielding his axe at the Battle of Bannockburn (Heritage Images).



Figure 2. A horseman's axe with a small blade and head size (Bonhams, 2012).



Figure 3. A horseman's axe on display in the Art Institute of Chicago (Art Institute Chicago, 2026).



Figure 4. An example of a horseman's axe with a large top spike (Incitatus, 2014).

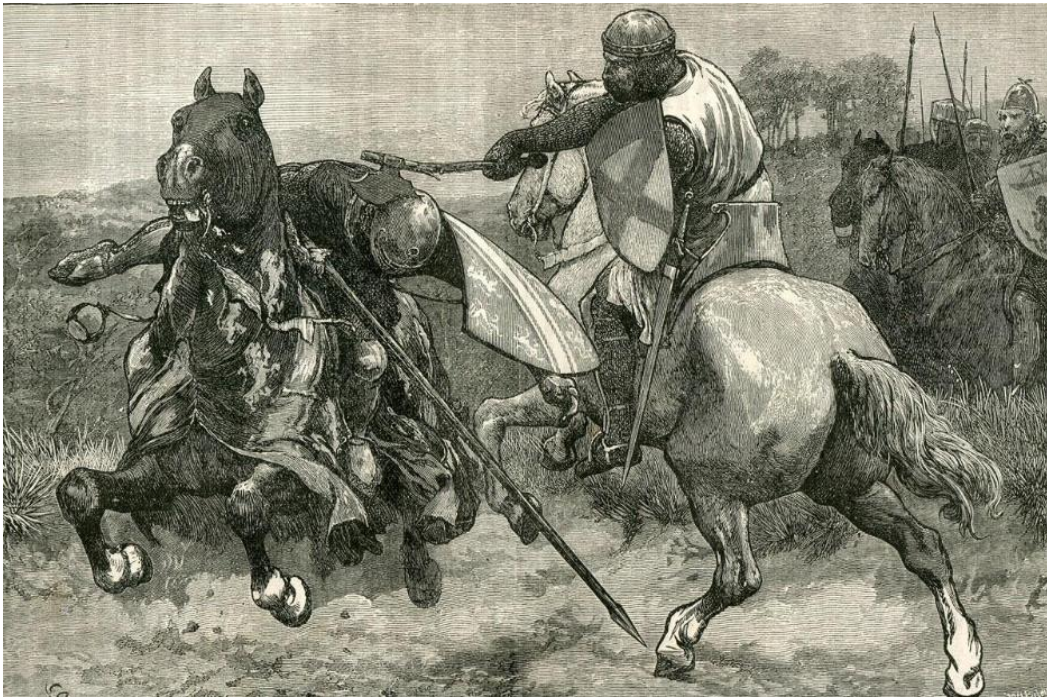


Figure 5. Robert the Bruce breaking his wooden handled axe while striking Sir Henry de Bohun (Hassall, 2025).

Table 1. The engineering requirements for the Steel Thunder team.

Need	Requirement	Unit	Value
1	Weight	Kilograms	≤ 1.5
2	Length	Millimeters	≤ 800
3	Casting Material	Pass/Fail	Steel
4	Multi-Implement Axe	Pass/Fail	Axe Head, Pick, Spike
5	Sharpness	BESS	≤ 250
6	Hardness	HRC	55 - 60
7	Edge Angle	Degrees	≤ 25
8	Industry Partner	Pass/Fail	Steel Foundry
9	Team Members	Student(s)	≤ 5
10	Video Documenting Progress	Minutes	≤ 5
11	Report Detailing Design and Process	Pages	≤ 10
12	Underclassman Helpers	Student(s)	≥ 2
13	Testing	Pass/Fail	Pre-Competition
14	Lab Safety	Pass/Fail	Full Compliance
15	Weekly Metal Pours	Pours Per Week	≥ 1
16	SDS Label Material	Pass/Fail	All Materials Labeled
17	Durability	Pass/Fail	Survives Competition
18	Recyclability	% of Weight	$> 80\%$ Recycled Metal

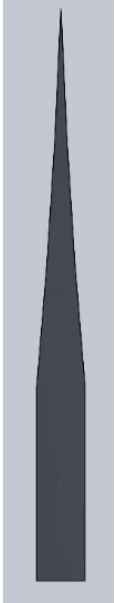

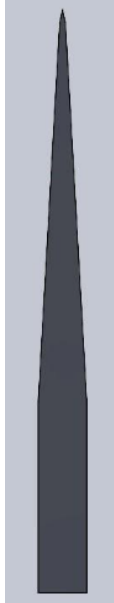
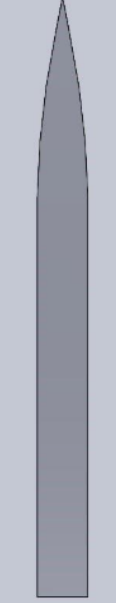
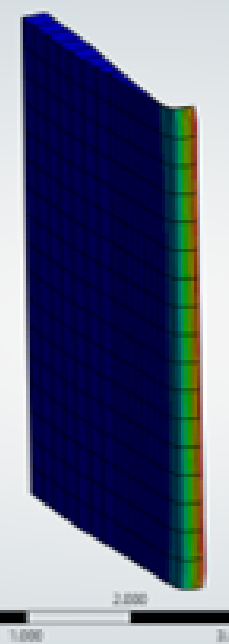
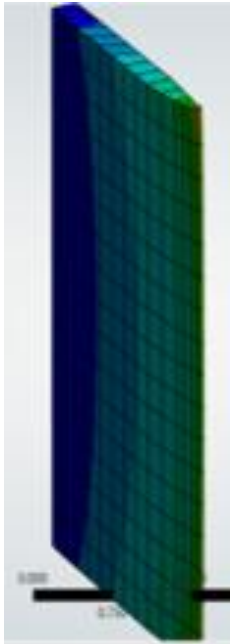
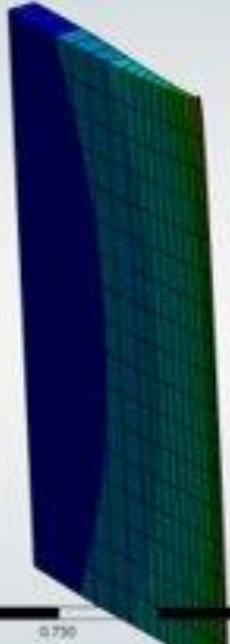
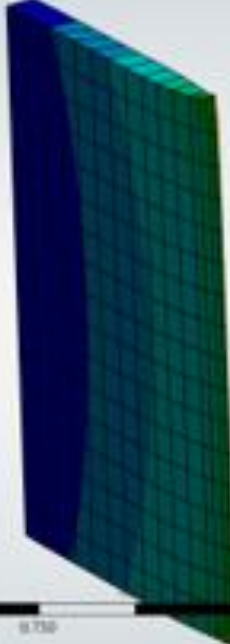


Figure 6. A wood handled horseman's axe at the Art Institute of Chicago (Art Institute of Chicago, n.d.).

Criteria	Weight	Hickory	Ash	Maple	Birch
Weight	30%	2	5	3	4
Durability	30%	5	4	3	2
Cost	15%	5	3	1	4
Historical Accuracy	25%	2	5	3	4
Total	100%	3.35	4.4	2.7	3.4

1 – Bad 2 – Poor 3 – Neutral 4 – Good 5 - Excellent
Figure 7. An example of one of the team's selection matrices for the handle wood type.

Table 2. Depictions of each edge grind type considered for the axe.

Hollow Edge Grind	Convex Edge Grind	Flat Edge Grind	Convex Grind with Hollow Grind Finish
 A 2D cross-sectional diagram of an axe head with a hollow edge grind. The grinding surface is concave, creating a hollowed-out profile along the cutting edge.	 A 2D cross-sectional diagram of an axe head with a convex edge grind. The grinding surface is curved outward, creating a rounded, convex profile along the cutting edge.	 A 2D cross-sectional diagram of an axe head with a flat edge grind. The grinding surface is a straight line, creating a flat profile along the cutting edge.	 A 2D cross-sectional diagram of an axe head with a convex grind that has a hollow grind finish. The grinding surface is convex but features a hollowed-out section near the tip.
 A 3D surface plot of the hollow edge grind. The surface is colored with a gradient from blue (low) to red (high). A scale bar at the bottom indicates a length of 1.000 units. The plot shows the concave curvature of the grinding surface.	 A 3D surface plot of the convex edge grind. The surface is colored with a gradient from blue (low) to red (high). A scale bar at the bottom indicates a length of 0.750 units. The plot shows the rounded, convex curvature of the grinding surface.	 A 3D surface plot of the flat edge grind. The surface is colored with a gradient from blue (low) to red (high). A scale bar at the bottom indicates a length of 0.750 units. The plot shows a flat, linear grinding surface.	 A 3D surface plot of the convex grind with hollow grind finish. The surface is colored with a gradient from blue (low) to red (high). A scale bar at the bottom indicates a length of 0.750 units. The plot shows the convex surface with a hollowed-out section.

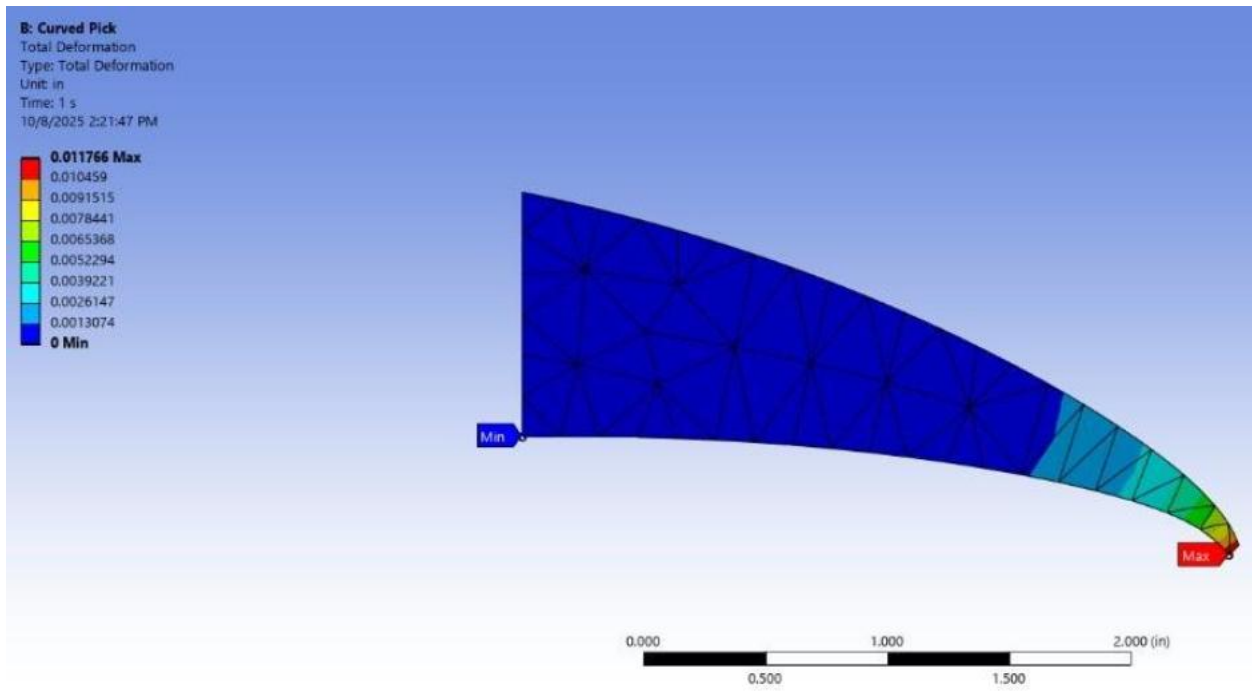


Figure 8. Finite element analysis during impact for the deformation of a curved pick.

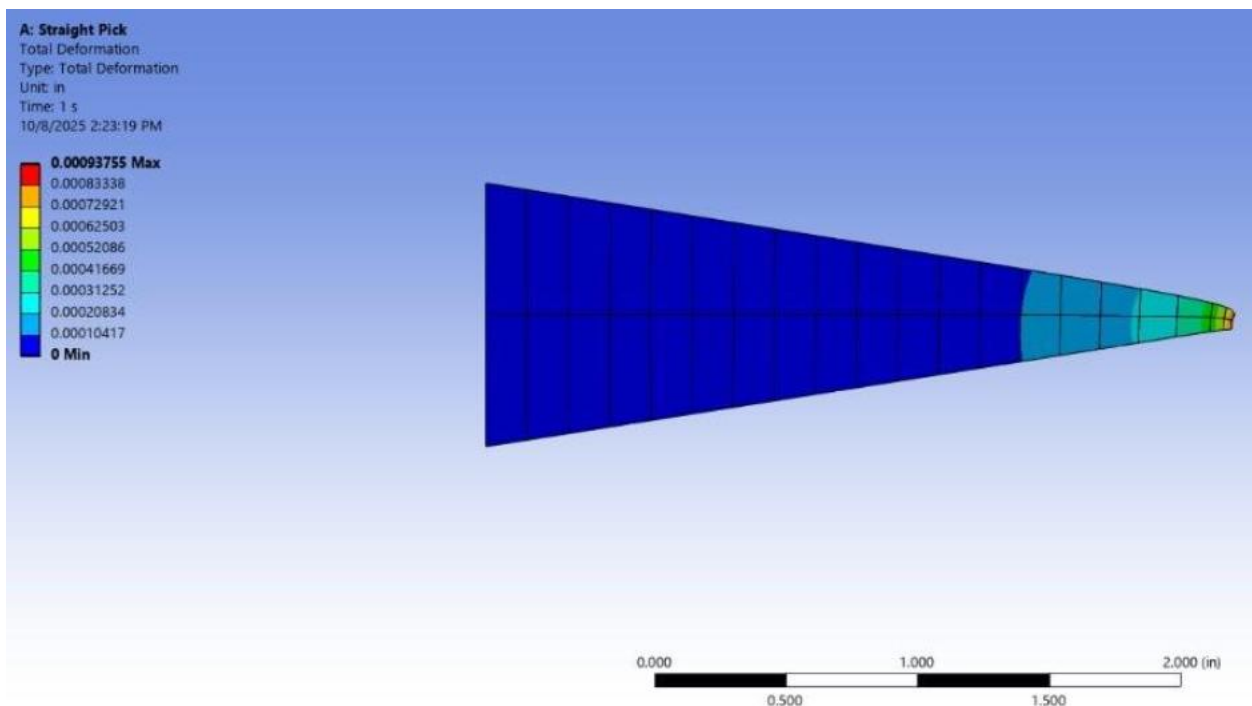


Figure 9. Finite element analysis during impact for the deformation of a straight pick.

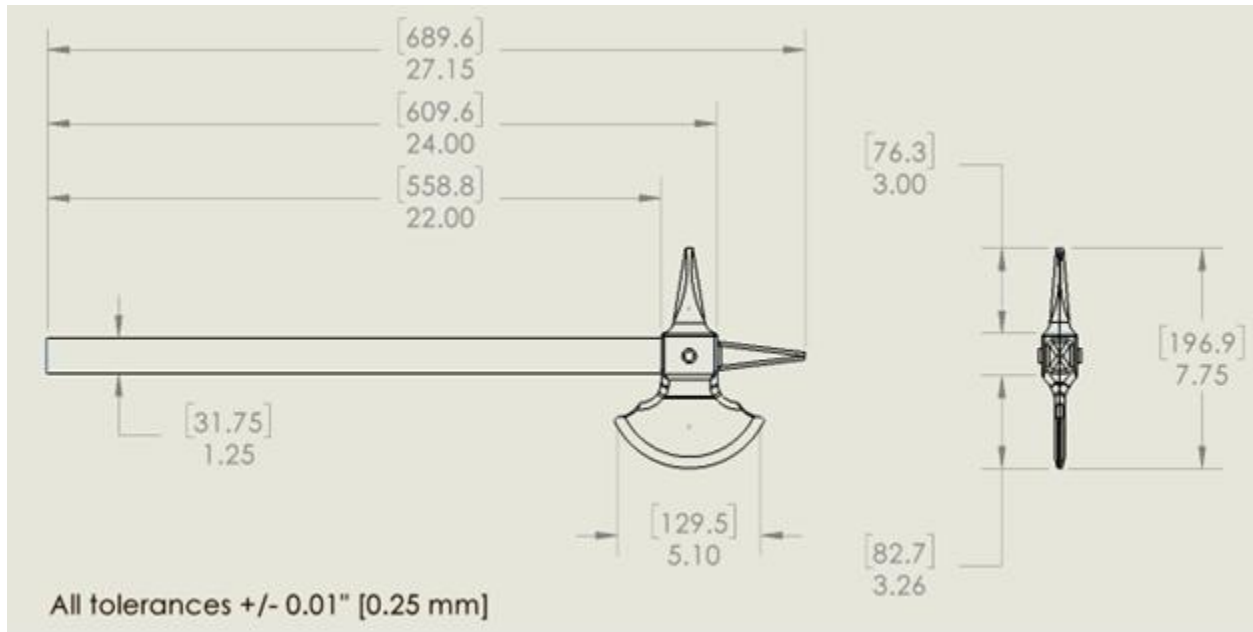


Figure 10. The CAD drawing of the final design, including preliminary dimensions.



Figure 11. A view of the computer model for the axe design.

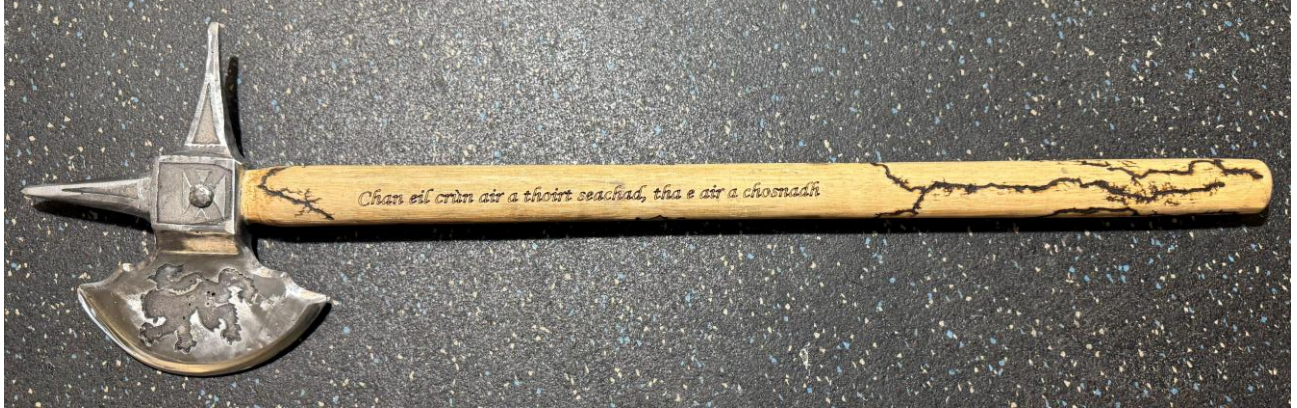


Figure 12. The full completed axe.



Figure 13. The etched, blued, and polished axe head.



Figure 14. The axe handle inscription.



Figure 15. The Lichtenberg figures that were burned into the handle of the axe.

Table 3. The percent composition ranges for AISI 4140 steel versus the final casting composition.

Element	% Composition of AISI 4140	% Composition of Casting
Carbon	0.38%-0.43%	0.394%
Silicon	0.15%-0.30%	0.172%
Manganese	0.75%-1%	0.75%
Phosphorus	<0.035%	0.018%
Sulfur	<0.04%	0.023%
Chromium	0.8%-1.1%	1.09%
Nickel	0-N/A	0.0036%
Molybdenum	0.15%-0.25%	0.159%

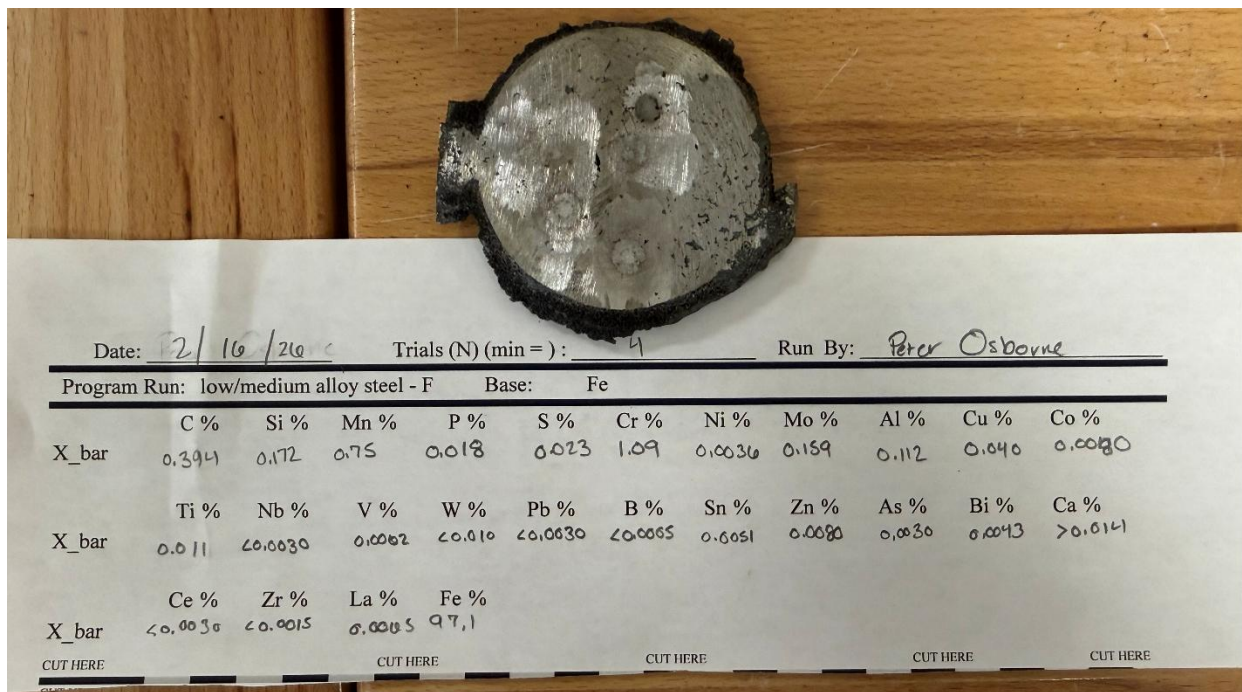


Figure 16. The arc spectrometer sample button and the data collection sheet for the final casting run in 4140 steel.



Figure 17. The refractory coating on the just-quenched axe head.

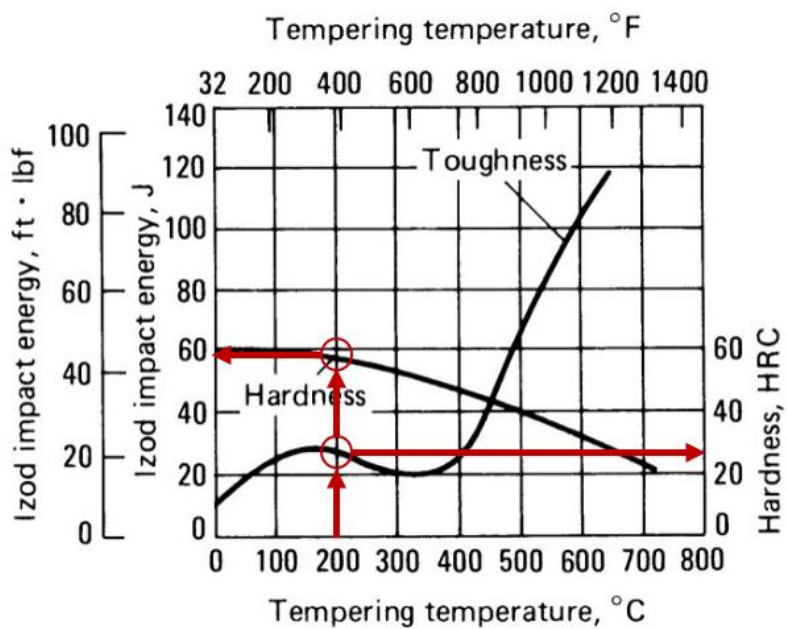


Figure 18. The tempering temperature versus hardness and toughness diagram (usmcpop, 2018).



Figure 19. The match plate for the final gating design.

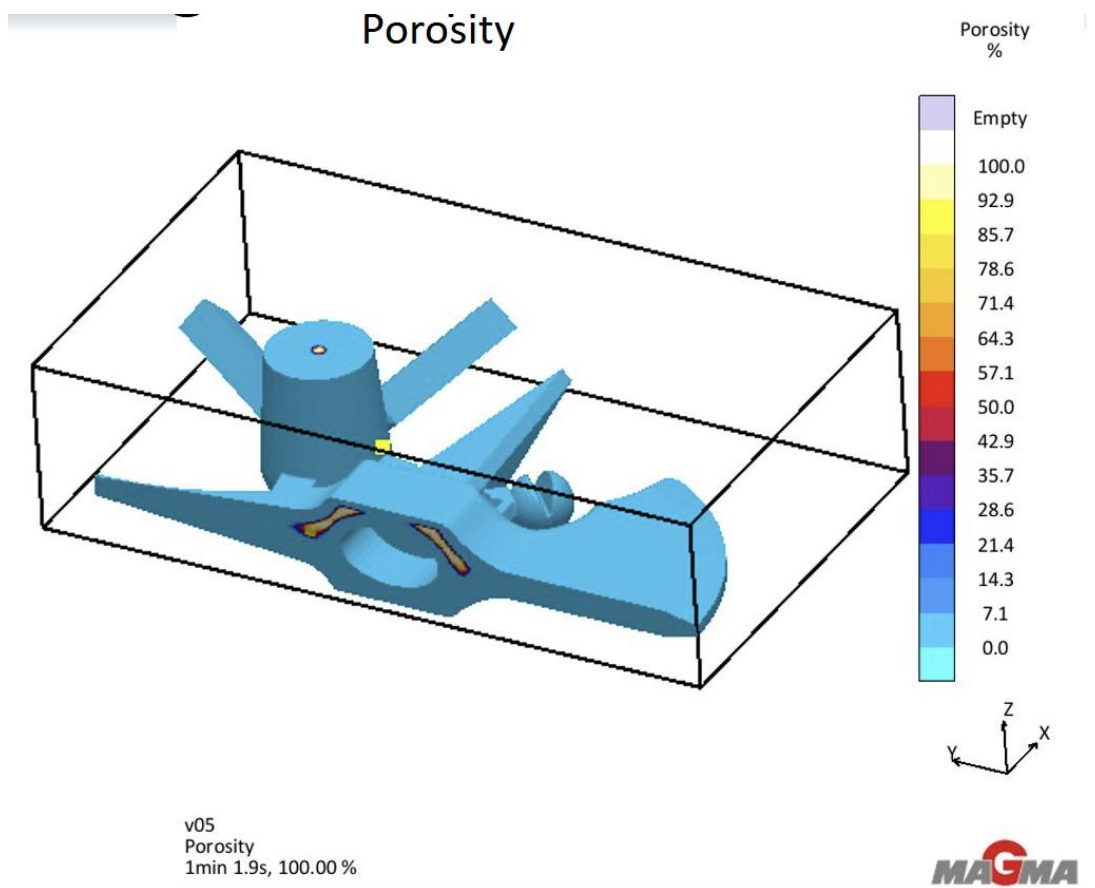


Figure 20. The porosity simulation in MAGMA, showing a higher likelihood of porosity on the upper half of the casting around the core.

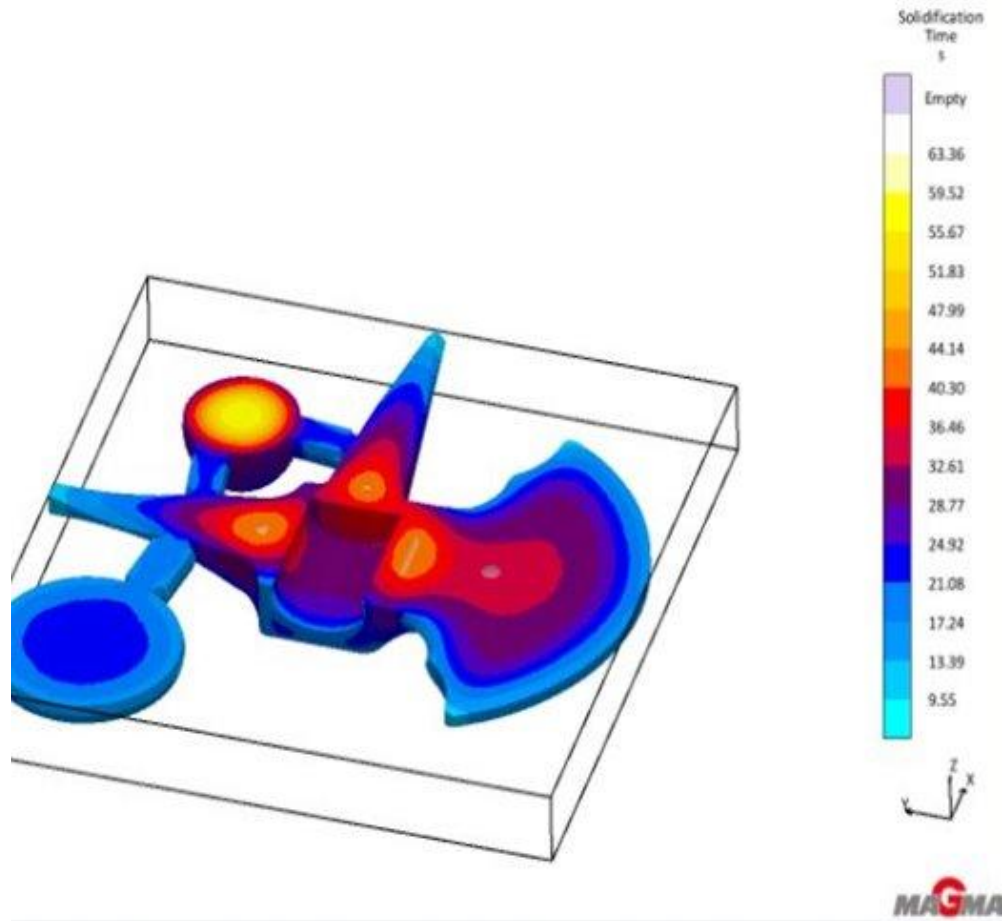


Figure 21. The solidification time for the MAGMA simulation of the final mold design, showing hot spots around the core.

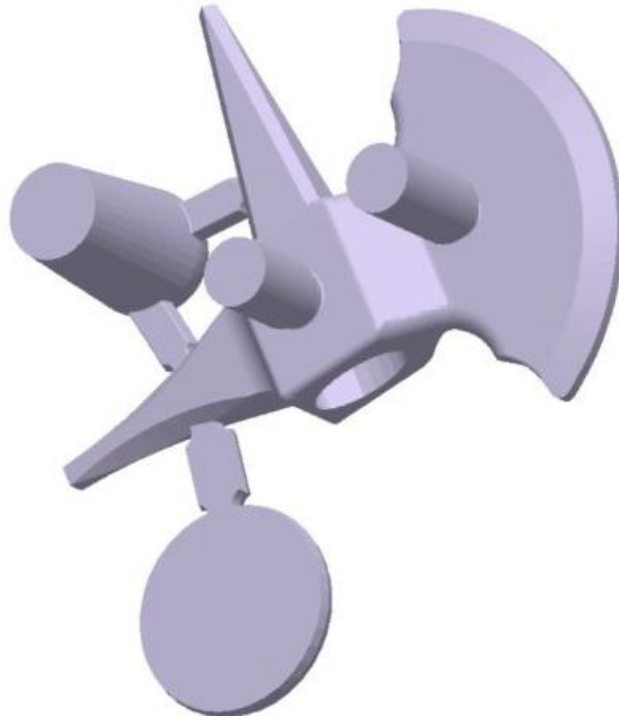


Figure 22. The final gating for the axe head, including two open air risers, a direct feed riser, and an arc spectrometer button.



Figure 23. An aluminum pour of the final gating iteration before degating and removal of the core sand.

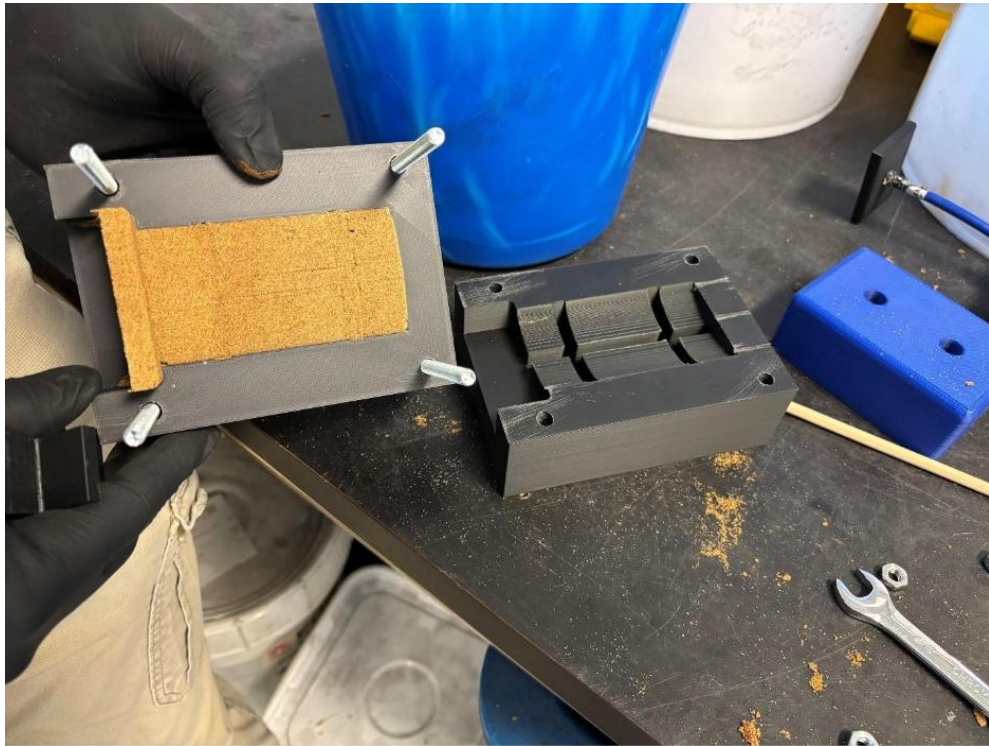


Figure 24. The core and core box for an early iteration of the axe.

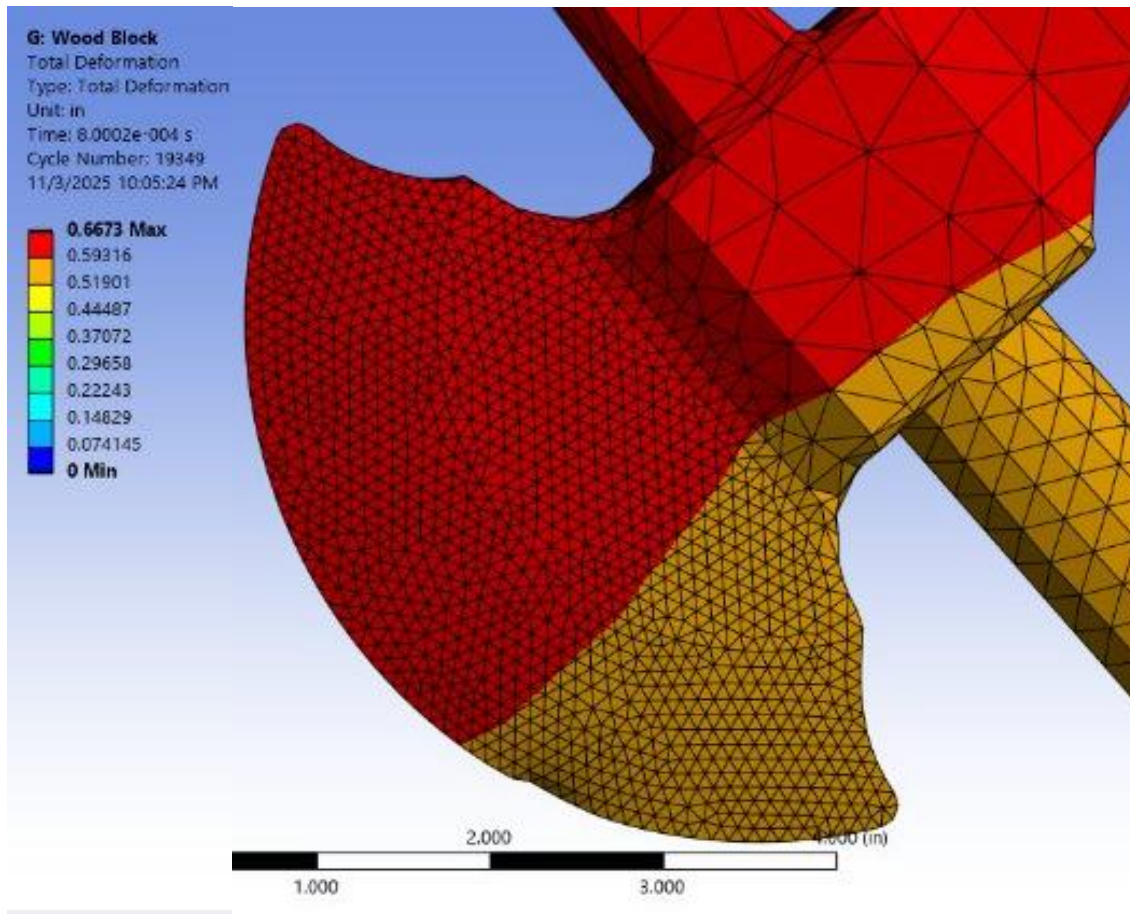


Figure 25. The simulated total deformation of the axe under a 150 mile per hour impact with an ice block.



Figure 26. The Charpy impact test specimens, with “true” 4140 on the left and cast 4140 on the right.

Table 4. The raw data from the Charpy impact testing.

Sample No.	“True” 4140	4140 Cast Bars	Notes
1	46.0 FT-LBS	19.0 FT-LBS	X
2	46.0 FT-LBS	18 FT-LBS	X
3	48.5 FT-LBS	220.0 FT-LBS	Oversized bar upon inspection, eliminated from calculations
4	46.5 FT-LBS	238.0 FT-LBS	
5	44.0 FT-LBS	54.0 FT-LBS	X
6	X	30.0 FT-LBS	X
7	X	27.5 FT-LBS	X
8	X	46.5 FT-LBS	X
9	X	130.0 FT-LBS	X
10	X	34.0 FT-LBS	X
AVERAGE	46.200 FT-LBS	44.875 FT-LBS	X
STD. DEVIATION	1.605 FT-LBS	36.577 FT-LBS	X

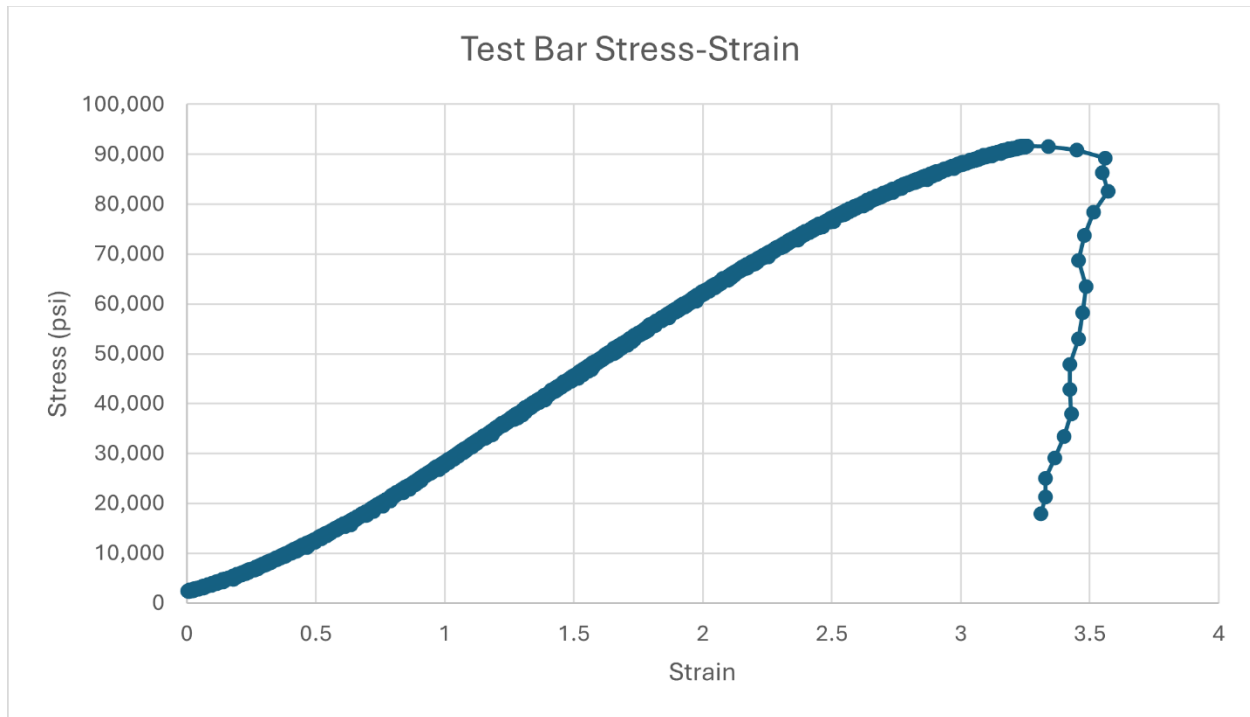


Figure 27. The stress-strain curve for one of the tensile bars pulled by Metal Technologies Auburn.

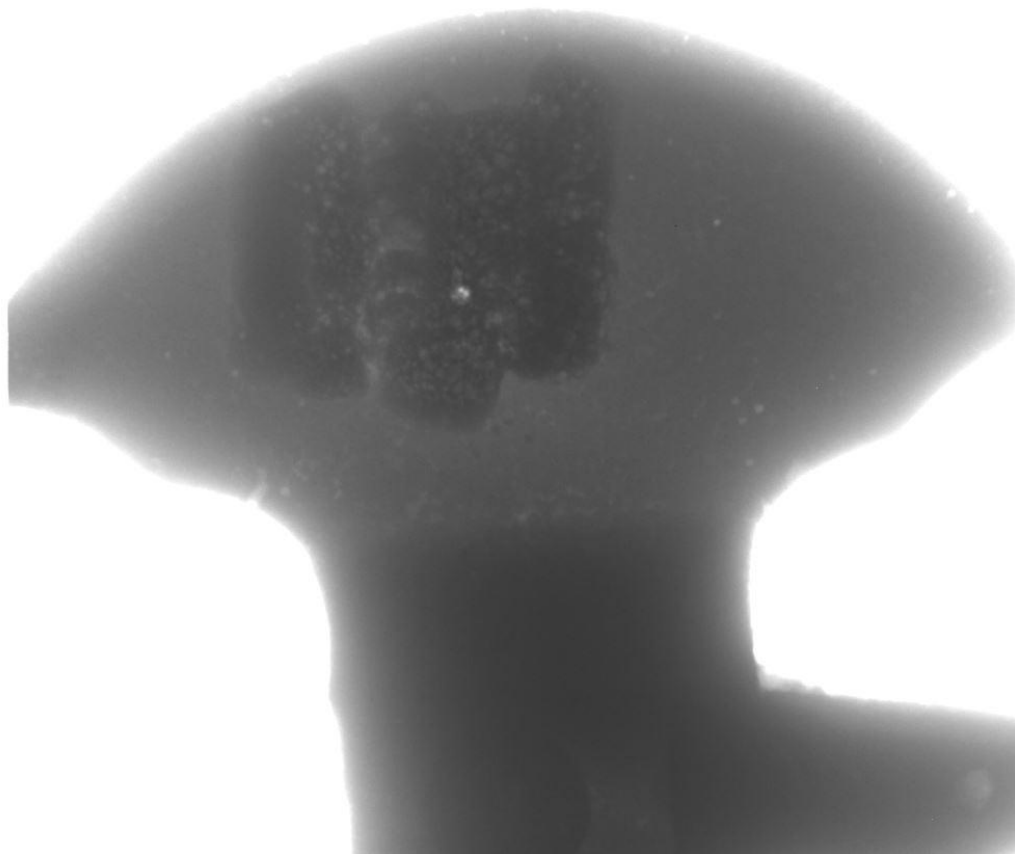


Figure 28. The blade X-ray for the weld-repaired testing axe.

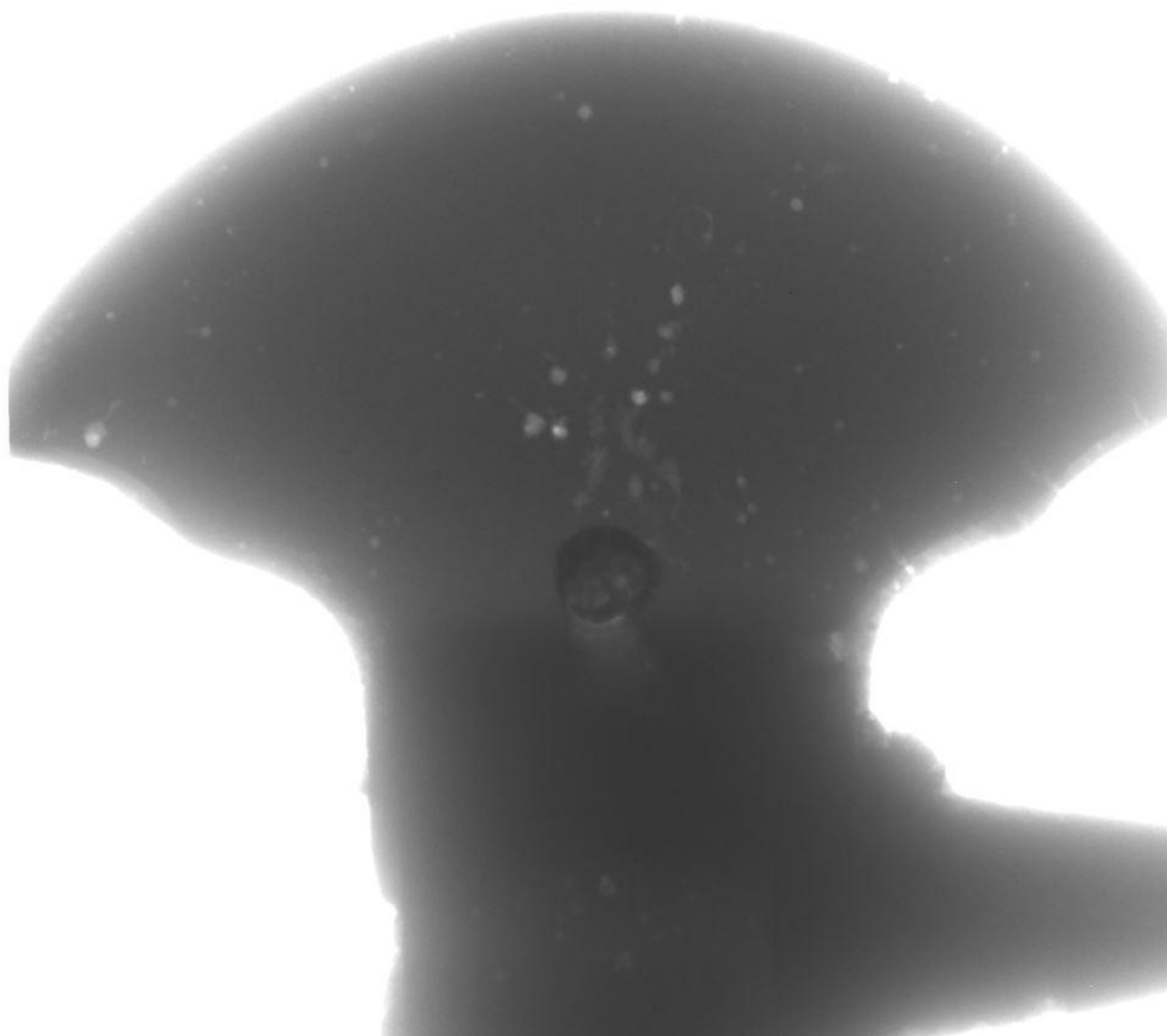


Figure 29. The blade X-ray for the competition axe.



Figure 30. The pick X-ray for the competition axe.

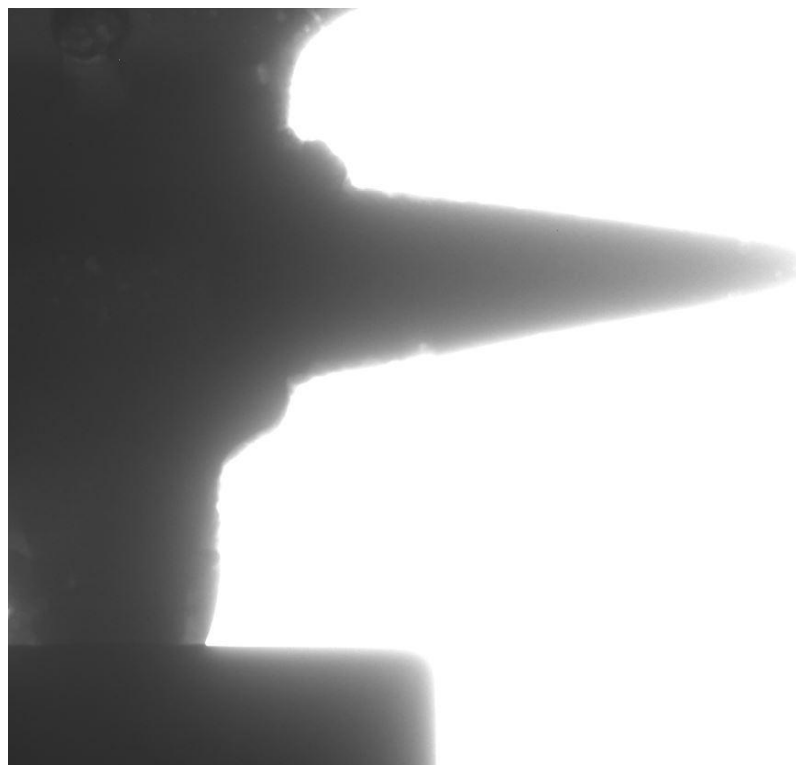


Figure 31. The top spike X-ray for the competition axe.

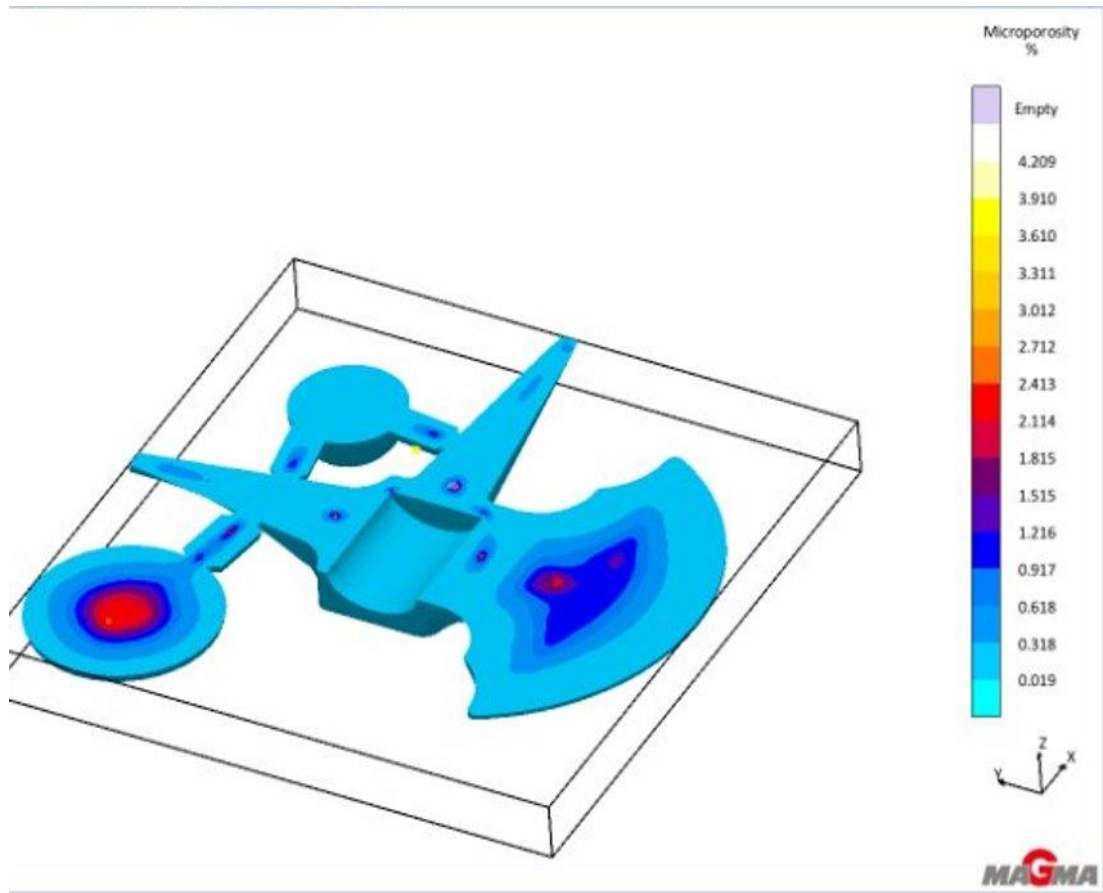


Figure 32. The MAGMA simulation of the final gating, depicting the nearly eliminated chances of microporosity in the final casting.

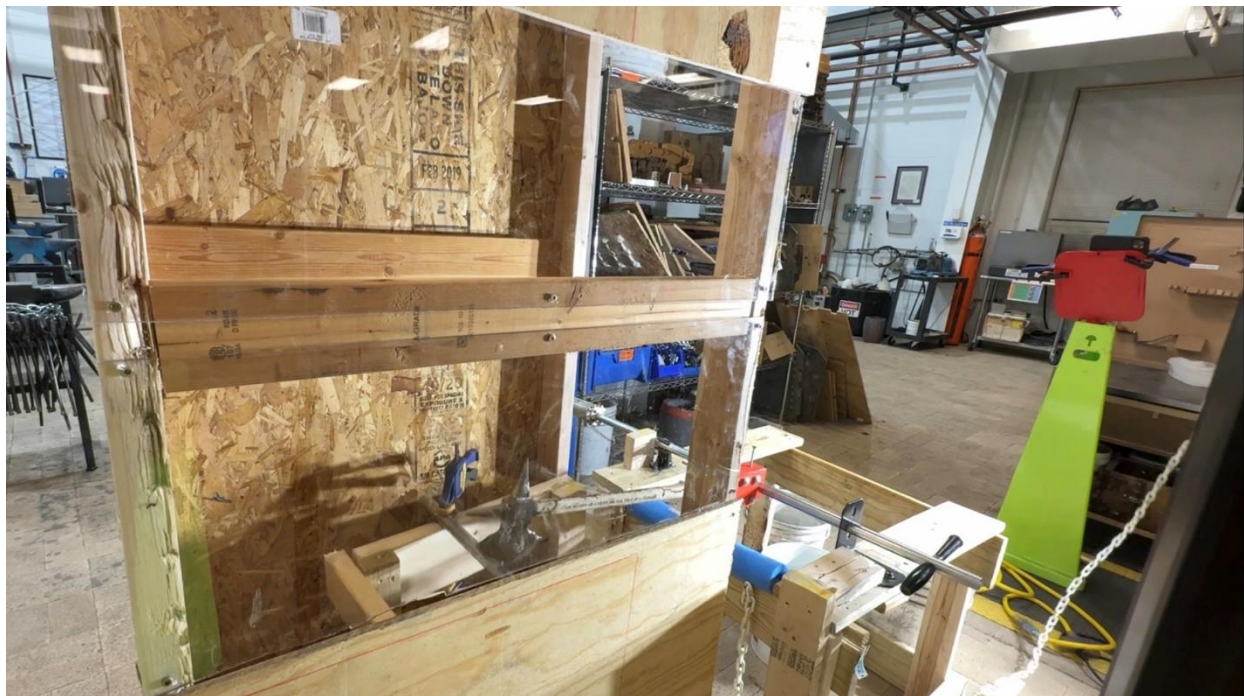


Figure 33. The testing rig chopping a piece of 16-gauge steel pipe.



Figure 34. The testing rig chopping an 18-gauge steel plate.



Figure 35. Hand testing the axe against the 18-gauge steel plate.



Figure 36. The second axe's blade after destructive testing, which showed slight dulling and rollover.



Figure 37. The second axe's pick after destructive testing, which showed no damage.



Figure 38. The 18-gauge steel plate after destructive testing.



Figure 39. Garrett enjoying fresh axe-sliced cantaloupe after successful destructive testing.



Figure 40. The trash can full of wood and cantaloupe scraps after destructive testing.